JACS
JOURNAL OF THE AMERICAN CHEMICAL SOCIETY

Communication

pubs.acs.org/JACS

Atomic Layer Deposition of Platinum Catalysts on Nanowire Surfaces for Photoelectrochemical Water Reduction

Neil P. Dasgupta,[†,⊥] Chong Liu,[†,‡,⊥] Sean Andrews,[†,‡] Fritz B. Prinz,[§] and Peidong Yang*[,†,‡,∥]

[†]Department of Chemistry and [‡]Department of Materials Science and Engineering, University of California, Berkeley, California 94720, United States

[§]Department of Mechanical Engineering, Stanford University, Stanford, California 94305, United States

[∥]Materials Science Division, Lawrence Berkeley National Laboratory, Berkeley, California 94720, United States

Supporting Information

ABSTRACT: The photocathodic hydrogen evolution reaction (HER) from p-type Si nanowire (NW) arrays was evaluated using platinum deposited by atomic layer deposition (ALD) as a HER cocatalyst. ALD of Pt on the NW surface led to a highly conformal coating of nanoparticles with sizes ranging from 0.5 to 3 nm, allowing for precise control of the Pt loading in deep submonolayer quantities. The catalytic performance was measured using as little as 1 cycle of Pt ALD, which corresponded to a surface mass loading of ∼10 ng/cm^2. The quantitative exploration of the lower limits of Pt cocatalyst loading reported here, and its application to high-surface-area NW photoelectrodes, establish a general approach for minimizing the cost of precious-metal cocatalysts for efficient and affordable solar-to-fuel applications.

Because of the intermittent nature of the solar resource, energy storage technologies are a critical component of a future renewable energy infrastructure. One attractive strategy is the direct storage of solar energy in the form of chemical bonds in a process known as artificial photosynthesis.[1] While the direct splitting of water can be achieved using a single wide-band-gap semiconductor, the overall thermodynamic efficiency of these systems is limited by insufficient light absorption.[2] To address this issue, a dual-band-gap system can be utilized,[3] in which the electrochemical half-reactions are separated into a semiconductor photoanode and photocathode, allowing for the use of lower-band-gap materials that can absorb a greater portion of the solar spectrum.

One of the issues during this solar-to-fuel process is the sluggish kinetics of the hydrogen evolution reaction (HER) at the semiconductor surface, which requires the incorporation of a cocatalyst material on the surface to reduce the reaction overpotential.[4] Among the various cocatalyst materials, noble metals such as Pt have been shown to provide the highest electrochemical activity toward the HER. However, the high cost of precious-metal cocatalysts limits the economic viability of an artificial photosynthesis scheme. While alternate cocatalyst materials based on earth-abundant elements are being explored to reduce the costs associated with the use of Pt[5] for solar-to-fuel applications, these materials still lag behind Pt in terms of electrochemical catalytic performance for the HER. An alternate approach to reducing the cocatalyst cost is to dramatically reduce the loading of Pt on the electrode surface while maintaining sufficient catalytic activity for the chemical reaction.

One way to reduce the required catalytic activity for a given overpotential is the use of high-surface-area photoelectrodes.[5a] In particular, one-dimensional semiconductor microwire and nanowire (NW) arrays are being explored for solar-to-fuel applications[6] because of their large semiconductor/electrolyte interfacial areas in addition to other beneficial properties, including enhanced light scattering and trapping[7] and efficient transport of charge carriers to the electrodes.[8] However, it remains challenging to apply a uniform coating of cocatalyst particles on these high-aspect-ratio structures using traditional deposition techniques such as electrodeposition or physical vapor deposition,[9] which can lead to poor utilization of the expensive Pt material. Therefore, a technique is needed to uniformly coat the surface of high-aspect-ratio structures with precise control of the catalyst loading and size to minimize the overall raw material cost.

One technique that meets this requirement is atomic layer deposition (ALD).[10] ALD is a modified chemical vapor deposition technique capable of conformal coating of ultra-high-aspect-ratio structures with subnanometer precision in material thickness due to self-limiting surface reactions and the separate introduction of material precursors in a cyclic manner. While many ALD processes lead to the formation of a dense thin film, certain reaction chemistries result in nucleation of isolated islands on the growth surface, which grow larger with increasing ALD cycle number and eventually coalesce into a film. This process has been explored for direct deposition of catalysts[11] and quantum dots[12] with diameters below 10 nm on nanostructured surfaces.

In this work, using a Si NW array photocathode as a model system with large surface area, we found that Pt nanoparticles (NPs) deposited by as little as one cycle of ALD can serve an efficient cocatalyst for photoelectrochemical water reduction. Pt NPs with diameters ranging from 0.5 to 3 nm were formed during the initial three ALD cycles, leading to a uniform catalyst loading along the length of the NW with a submonolayer Pt surface density. Electrochemical and photoelectrochemical

Received: June 6, 2013
Published: August 20, 2013

   dx.doi.org/10.1021/ja405680p | J. Am. Chem. Soc. 2013, 135, 12932−12935

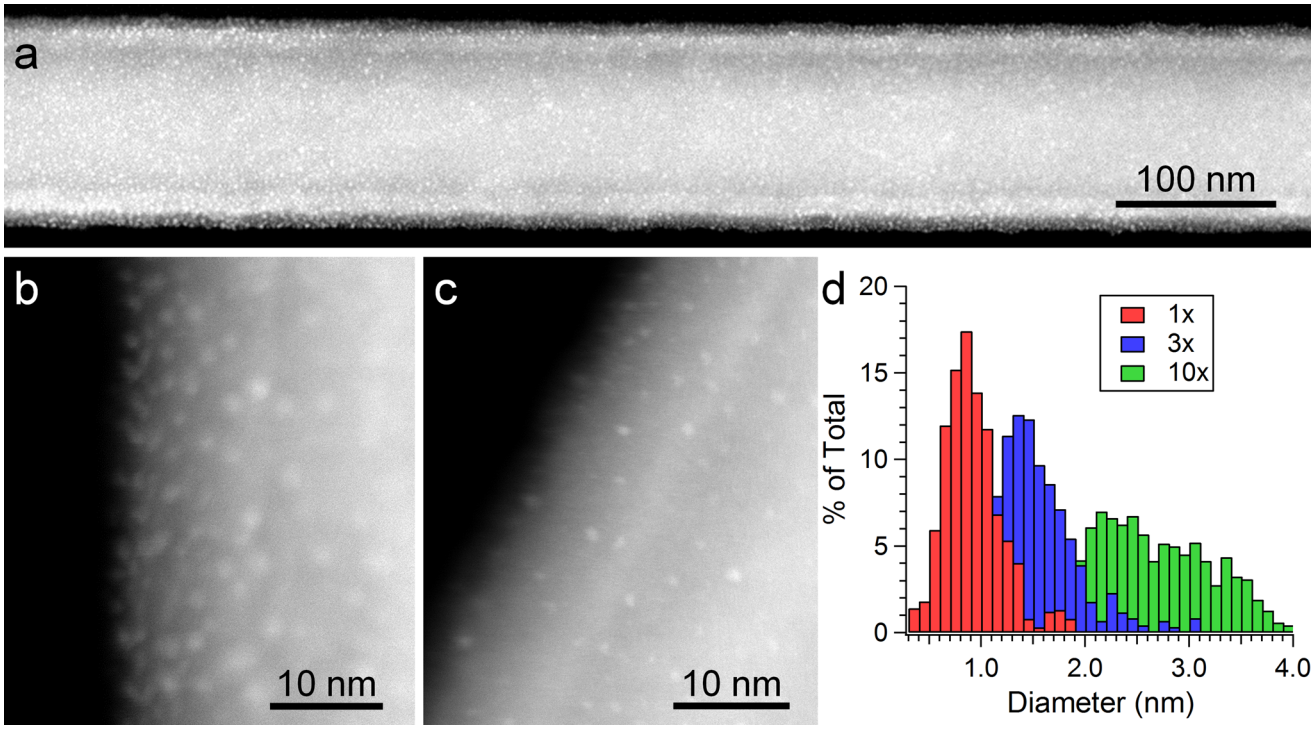

Figure 1. STEM analysis of Pt NPs deposited on Si/TiO_2 core–shell NWs by ALD. (a–c) High-angle annular dark-field STEM images of a NW after (a) 10 cycles, (b) 3 cycles, and (c) 1 cycle of Pt ALD. The low-magnification image in (a) shows a core–shell NW coated with a uniform coverage of discrete Pt NPs. (d) Histogram of particle size for various numbers of cycles.

measurements demonstrated that the HER catalytic activity of these Pt clusters on high-surface-area NW photoelectrodes is stable and sufficient for solar-to-fuel applications. The combination of highly uniform coating and precise control of the NP size and loading in the ALD process is a powerful tool that can take advantage of the benefits of the NW geometry while minimizing the total volume of Pt required.

P-type Si NW arrays were selected as a photocathode material because they have a suitable conduction band edge with respect to the HER potential and a sufficiently low band gap for absorption of visible light.[4a] The well-defined NW arrays [see the Supporting Information (SI)] provide a high-surface-area structure suitable for quantitative analysis. To achieve a positive photovoltage and stabilize the Si surface, a p-Si/TiO_2 core–shell structure was formed by ALD of 10–12 nm TiO_2 on the NW surface, which was followed by deposition of Pt by ALD.[13]

The morphology of the core–shell p-Si/TiO_2 NWs loaded with Pt NPs was observed using aberration-corrected scanning transmission electron microscopy (STEM). Nucleation of subnanometer-scale islands on the NW surface was observed after only one ALD cycle (Figure 1c). Low-magnification STEM analysis demonstrated the excellent uniformity of the ALD coatings along the length of the NW surface (Figure 1a). This was further confirmed by high-magnification STEM analysis of different regions of a NW after one ALD cycle (see the SI). A high-resolution image of a single 2 nm Pt NP showed a crystalline phase with a *d* spacing of 2.3 Å (see the SI). A histogram of the lateral dimensions of the islands based on several images is shown in Figure 1d. We measured an average particle diameter of 0.8 nm after one cycle, with a standard deviation of 0.25 nm. The size and density of the Pt NPs on the surface increased with the number of ALD cycles, showing that the Pt loading and particle size can be controlled by simply varying the number of cycles. We note that the STEM images over-represent the absolute value of surface particle density because of the curved surface of the NW and the fact that nanoclusters on both sides of the NW appear in the images.

It is well-known that Pt ALD exhibits a nonlinear nucleation phase during the initial cycles[11c,f,h] that is highly dependent on the ALD conditions and surface chemistry of the substrate.[14] The exact nucleation mechanisms are still a matter of intense research.[15] The formation of clusters in this size range suggests that surface diffusion of Pt atoms occurs during the initial cycles, leading to a sparse distribution of Pt clusters on the surface rather than a uniform monolayer of atoms. Further research into these nucleation and surface diffusion phenomena in the future is likely to improve the ability to control the size and density of the Pt clusters with greater precision.

To provide a more quantitative measure of the surface coverage, total-reflection X-ray fluoresecence (TXRF) was performed on a planar Si wafer coated under the same ALD conditions (see the SI). After one cycle of Pt ALD, the surface coverage was measured to be $(4.0 \pm 0.5) \times 10^{13}$ cm^{-2}, corresponding to a surface density of ~2.7% relative to the Pt(111) surface (1.5×10^{15} cm^{-2}) and a platinum mass loading of ~10 ng/cm^2, which is consistent with the STEM analysis of the NW surface (see the SI). Therefore, while the atomic-scale distribution of Pt atoms on the surface was not homogeneous because of the formation of Pt clusters, the cocatalyst loading via ALD was in the deep submonolayer level. Furthermore, in shallow-angle X-ray photoelectron spectroscopy (XPS) measurements, an increase in the peak intensity was observed as the number of ALD cycles increased, showing a monotonic increase in the Pt loading with the number of cycles (see the SI). These low levels of uniform Pt loading over a high-aspect-ratio surface, which would be extremely difficult to achieve by

dx.doi.org/10.1021/ja405680p | J. Am. Chem. Soc. 2013, 135, 12932–12935

standard Pt deposition techniques, allowed us to efficiently explore the lower limits of Pt loading for catalytic activity of the HER reaction.

The electrocatalytic performance of the Pt NPs was tested using planar fluorine-doped tin oxide (FTO) substrates as electrodes (see the SI). A 12 nm layer of TiO_2 was first deposited on the FTO surface, followed by Pt deposition using various numbers of ALD cycles to replicate the conditions on the p-Si NWs. The catalytic performance was measured using linear sweep voltammetry in 0.5 M H_2SO_4 electrolyte, with series resistance subtracted, under a standard three-electrode configuration. The measured onset of a cathodic current at a potential negative of 0 V vs reversible hydrogen electrode (RHE) (Figure 2a) and the observed formation of gas bubbles

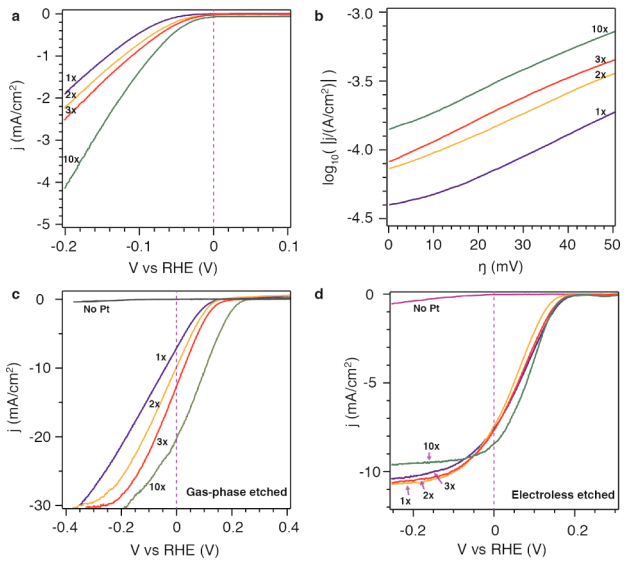

Figure 2. (a, b) Electrochemical and (c, d) photoelectrochemical performance of Pt cocatalysts loaded via ALD in 0.5 M H_2SO_4 electrolyte. (a) Linear sweep voltammograms and (b) Tafel plots for TiO_2-coated FTO substrates with Pt deposited using various numbers of ALD cycles. (c) HER performance (under 1 sun illumination) of Si NW array photocathodes synthesized via gas-phase etching and loaded with ALD Pt cocatalyst. (d) HER performance of a Si NW photocathode synthesized via electroless etching under the same condition as in (c).

at high current density implied catalytic activity for the HER. The cathodic currents increased with increasing number of Pt ALD cycles, consistent with the confirmed increase of the Pt loading. All of the samples exhibited a current slope of ~60 mV per decade in the Tafel plots (Figure 2b), from which the apparent exchange current densities (j_0) were obtained for substrates formed using different numbers of ALD cycles (Table 1).

In the case of high-surface-area structures, the required catalytic activity is reduced because of the lower actual current density on the surface. Therefore, the ability to precisely control the Pt loading in this submonolayer regime allows for an exploration of the lower limits of platinum usage required in high-aspect-ratio structures. To explore this hypothesis, the photoelectrochemical (PEC) performance of these Pt catalysts on Si NW array photocathodes was tested.

A well-defined high-surface-area Si NW array electrode was synthesized via gas-phase deep reactive ion etching (DRIE) (see the SI). The PEC performance of these photocathodes was

Table 1. Summary of Electrochemical and Photoelectrochemical Performance of Pt Catalysts Formed by ALD

no. of cycles	surface Pt loading (ng/cm^2)	j_0 (μA/cm^2)	j_{sc} (mA/cm^2)[a]
1	13 ± 3	27 ± 4	7.1
2	24 ± 5	59 ± 9	8.3
3	34 ± 7	85 ± 10	12.5
10	105 ± 21	130 ± 20	20.7

[a]Current density at 0 V vs RHE.

tested under the same conditions as in the electrochemical measurements described above. It was empirically found that the thin TiO_2 interlayer was required to achieve positive photovoltages with these ALD Pt catalysts on the Si surface. A similar phenomenon was observed in electron-beam-evaporated Pt catalysts on bare Si, which was attributed to the formation of an Ohmic contact between Si and Pt that determined the energetics of the Si–Pt-electrolyte interface.[5a] However, the presence of an intermediate TiO_2 barrier layer allowed for the observation of a characteristic photocathode j–V curve with as little as one ALD cycle, despite the ultralow Pt loading under these conditions. The Si NW photocathode exhibited no photoactivity in the absence of Pt cocatalyst (Figure 2c). For all of the samples measured, an onset voltage of 0.15–0.25 V vs RHE and current densities of ~30 mA/cm^2 were observed under 100 mW/cm^2 simulated AM 1.5 irradiation.

Moreover, the slope of the j–V curve was seen to increase as the number of ALD cycles was increased from 1 to 10, leading to an increase in the current density at 0 V vs RHE (j_{sc}) from 7 to 21 mA/cm^2, which is comparable to previous results for p-Si wires using standard Pt processing techniques.[5a] This indicates that the HER catalytic activity of the Pt atoms on the NW surface determines the slope of the j–V curve. Table 1 shows a comparison of the surface loading of Pt (calculated from the TXRF and XPS data) with the electrochemical and photoelectrochemical performance of the ALD Pt catalysts (for further details, see the SI).

These results demonstrate the ability to tune the catalytic activity of the Pt NPs simply by varying the number of ALD cycles, while maintaining very low levels of Pt loading. For an affordable application of overall water splitting by coupling of two light-absorbing semiconductors, a current density on the order of 10 mA/cm^2 is expected.[4a] The photocathode obtained using one Pt ALD cycle provided a current density of ~7 mA/cm^2 at 0 V vs RHE, indicating that the use of ALD for Pt cocatalyst loading is applicable to an affordable integrated water-splitting system.

To study the impact of the NW surface area on the required catalytic activity, the ALD TiO_2/Pt coatings were deposited on electroless-etched NW arrays with a higher surface roughness factor than the gas-phase-etched NWs (for synthesis details, see the SI). Increasing the surface area should decrease the surface flux of electrons, leading to a lower requirement of catalytic activity on the surface. Because of the high surface area of these structures, the j–V behavior of the arrays did not vary significantly even when only one ALD cycle was used (Figure 2d). On the other hand, use of the electroless-etched NW arrays led to a decrease in photocurrent, which could be due to increased surface recombination for these larger surface areas. Therefore, while further decreasing the NW diameter may decrease the catalyst activity and material purity requirements because of the increased surface area and decreased minority

dx.doi.org/10.1021/ja405680p | J. Am. Chem. Soc. 2013, 135, 12932–12935

carrier diffusion length requirement, there is an optimal diameter below which the additional surface area will begin to have a detrimental effect on the performance of NW array photoelectrodes.

Another important consideration for PEC energy conversion is the stability of the photoelectrode under illumination in the electrolyte solution. Si photocathodes are known to suffer from degradation under operating conditions, which is attributed to oxidation of the Si surface. Recently, thin TiO_2 layers have been shown to stabilize the Si surface against oxidation, which is due to efficient electronic transport through the TiO_2 layer.[16] The photocurrent in our core−shell NW was measured to be stable with no measurable degradation after 1 h of illumination in solution (see the SI), suggesting that the thin TiO_2 interfacial layer provided the additional benefit of stabilizing the semiconductor surface. Further optimization of this interfacial layer to maximize the onset voltage and stability of this system is currently being investigated.

In this study, we have quantitatively analyzed the catalytic activity of submonolayer Pt NPs deposited by ALD. Catalytic activity was observed for as little as one ALD cycle, corresponding to a surface coverage of $\sim 4 \times 10^{13}$ atoms/cm^2. The photoelectrochemical catalytic performance of these NPs was evaluated on NW surfaces, providing a quantitative exploration of the lower limits of Pt loading on high-surface-area electrodes. The ALD technique facilitates uniform coverage of high-aspect-ratio surfaces with these ultralow Pt loadings, which could potentially reduce the costs associated with use of noble-metal catalysts. Additionally, the presence of an interfacial TiO_2 layer was found to be important to improve the photovoltage and stability of these Pt-coated NW arrays.

■ ASSOCIATED CONTENT

Supporting Information

Experimental details, additional TEM and SEM data, stability measurement, and calculations of electrochemical performance. This material is available free of charge via the Internet at http://pubs.acs.org.

■ AUTHOR INFORMATION

Corresponding Author

p_yang@berkeley.edu

Author Contributions

⊥N.P.D. and C.L. contributed equally.

Notes

The authors declare no competing financial interest.

■ ACKNOWLEDGMENTS

N.P.D. acknowledges support from the U.S. Department of Energy through an Office of Energy Efficiency and Renewable Energy (EERE) Postdoctoral Research Award under the SunShot Solar Energy Technologies Program. This work was supported by the Director, Office of Science, Office of Basic Energy Sciences, Materials Sciences and Engineering Division, U.S. Department of Energy under Contract No. DE-AC02-05CH11231.

■ REFERENCES

(1) (a) Lewis, N. S.; Nocera, D. G. *Proc. Natl. Acad. Sci. U.S.A.* **2006**, *103*, 15729. (b) Listorti, A.; Durrant, J.; Barber, J. *Nat. Mater.* **2009**, *8*, 929. (c) Bard, A. J.; Fox, M. A. *Acc. Chem. Res.* **1995**, *28*, 141.

(2) Bolton, J. R.; Strickler, S. J.; Connolly, J. S. *Nature* **1985**, *316*, 495.

(3) (a) Ohashi, K.; McCann, J.; Bockris, J. O. M. *Nature* **1977**, *266*, 610. (b) Nozik, A. J. *Appl. Phys. Lett.* **1976**, *29*, 150. (c) Kudo, A. *MRS Bull.* **2011**, *36*, 32.

(4) (a) Walter, M. G.; Warren, E. L.; McKone, J. R.; Boettcher, S. W.; Mi, Q.; Santori, E. A.; Lewis, N. S. *Chem. Rev.* **2010**, *110*, 6446. (b) Skúlason, E.; Tripkovic, V.; Björketun, M. E.; Gudmundsdóttir, S.; Karlberg, G.; Rossmeisl, J.; Bligaard, T.; Jónsson, H.; Nørskov, J. K. *J. Phys. Chem. C* **2010**, *114*, 18182.

(5) (a) McKone, J. R.; Warren, E. L.; Bierman, M. J.; Boettcher, S. W.; Brunschwig, B. S.; Lewis, N. S.; Gray, H. B. *Energy Environ. Sci.* **2011**, *4*, 3573. (b) Hou, Y.; Abrams, B. L.; Vesborg, P. C. K.; Björketun, M. E.; Herbst, K.; Bech, L.; Setti, A. M.; Damsgaard, C. D.; Pedersen, T.; Hansen, O.; Rossmeisl, J.; Dahl, S.; Nørskov, J. K.; Chorkendorff, I. *Nat. Mater.* **2011**, *10*, 434. (c) Hinnemann, B.; Moses, P. G.; Bonde, J.; Jørgensen, K. P.; Nielsen, J. H.; Horch, S.; Chorkendorff, I.; Nørskov, J. K. *J. Am. Chem. Soc.* **2005**, *127*, 5308. (d) Chen, Z.; Cummins, D.; Reinecke, B. N.; Clark, E.; Sunkara, M. K.; Jaramillo, T. F. *Nano Lett.* **2011**, *11*, 4168. (e) Warren, E. L.; McKone, J. R.; Atwater, H. A.; Gray, H. B.; Lewis, N. S. *Energy Environ. Sci.* **2012**, *5*, 9653.

(6) (a) Yang, P. *MRS Bull.* **2012**, *37*, 806. (b) Boettcher, S. W.; Warren, E. L.; Putnam, M. C.; Santori, E. A.; Turner-Evans, D.; Kelzenberg, M. D.; Walter, M. G.; McKone, J. R.; Brunschwig, B. S.; Atwater, H. A.; Lewis, N. S. *J. Am. Chem. Soc.* **2011**, *133*, 1216.

(7) (a) Garnett, E.; Yang, P. *Nano Lett.* **2010**, *10*, 1082. (b) Kelzenberg, M. D.; Boettcher, S. W.; Petykiewicz, J. A.; Turner-Evans, D. B.; Putnam, M. C.; Warren, E. L.; Spurgeon, J. M.; Briggs, R. M.; Lewis, N. S.; Atwater, H. A. *Nat. Mater.* **2010**, *9*, 239. (c) Hu, L.; Chen, G. *Nano Lett.* **2007**, *7*, 3249.

(8) (a) Kayes, B. M.; Atwater, H. A.; Lewis, N. S. *J. Appl. Phys.* **2005**, *97*, No. 114302. (b) Law, M.; Greene, L. E.; Johnson, J. C.; Saykally, R.; Yang, P. D. *Nat. Mater.* **2005**, *4*, 455.

(9) Oh, I.; Kye, J.; Hwang, S. *Nano Lett.* **2012**, *12*, 298.

(10) George, S. M. *Chem. Rev.* **2010**, *110*, 111.

(11) (a) Elam, J. W.; Dasgupta, N. P.; Prinz, F. B. *MRS Bull.* **2011**, *36*, 899. (b) Liu, C.; Wang, C. C.; Kei, C. C.; Hsueh, Y. C.; Perng, T. P. *Small* **2009**, *5*, 1535. (c) King, J. S.; Wittstock, A.; Biener, J.; Kucheyev, S. O.; Wang, Y. M.; Baumann, T. F.; Giri, S. K.; Hamza, A. V.; Baeumer, M.; Bent, S. F. *Nano Lett.* **2008**, *8*, 2405. (d) Christensen, S. T.; Feng, H.; Libera, J. L.; Guo, N.; Miller, J. T.; Stair, P. C.; Elam, J. W. *Nano Lett.* **2010**, *10*, 3047. (e) Feng, H.; Elam, J. W.; Libera, J. A.; Setthapun, W.; Stair, P. C. *Chem. Mater.* **2010**, *22*, 3133. (f) Christensen, S. T.; Elam, J. W.; Rabuffetti, F. A.; Ma, Q.; Weigand, S. J.; Lee, B.; Seifert, S.; Stair, P. C.; Poeppelmeier, K. R.; Hersam, M. C.; Bedzyk, M. J. *Small* **2009**, *5*, 750. (g) Hsu, I. J.; Kimmel, Y. C.; Jiang, X.; Willis, B. G.; Chen, J. G. *Chem. Commun.* **2012**, *48*, 1063. (h) Chao, C.-C.; Motoyama, M.; Prinz, F. B. *Adv. Energy Mater.* **2012**, *2*, 651.

(12) Dasgupta, N. P.; Jung, H. J.; Trejo, O.; McDowell, M. T.; Hryciw, A.; Brongersma, M.; Sinclair, R.; Prinz, F. B. *Nano Lett.* **2011**, *11*, 934.

(13) Aaltonen, T.; Ritala, M.; Sajavaara, T.; Keinonen, J.; Leskela, M. *Chem. Mater.* **2003**, *15*, 1924.

(14) Lee, H. B. R.; Bent, S. F. *Chem. Mater.* **2012**, *24*, 279.

(15) (a) Aaltonen, T.; Rahtu, A.; Ritala, M.; Leskela, M. *Electrochem. Solid-State Lett.* **2003**, *6*, C130. (b) Elliott, S. D. *Langmuir* **2010**, *26*, 9179. (c) Mackus, A. J. M.; Leick, N.; Baker, L.; Kessels, W. M. M. *Chem. Mater.* **2012**, *24*, 1752.

(16) Seger, B.; Pedersen, T.; Laursen, A. B.; Vesborg, P. C. K.; Hansen, O.; Chorkendorff, I. *J. Am. Chem. Soc.* **2013**, *135*, 1057.